Monopole-Driven Shell Evolution below the Doubly Magic Nucleus ^{132}Sn Explored with the Long-Lived Isomer in ^{126}Pd

H. Watanabe,[1,2,*] G. Lorusso,[2] S. Nishimura,[2] T. Otsuka,[3,4] K. Ogawa,[2] Z. Y. Xu,[3] T. Sumikama,[5] P.-A. Söderström,[2] P. Doornenbal,[2] Z. Li,[6] F. Browne,[2,7] G. Gey,[2,8] H. S. Jung,[9,†] J. Taprogge,[2,10,11] Zs. Vajta,[2,12] J. Wu,[2,6] A. Yagi,[13] H. Baba,[2] G. Benzoni,[14] K. Y. Chae,[15] F. C. L. Crespi,[14,16] N. Fukuda,[2] R. Gernhäuser,[17] N. Inabe,[2] T. Isobe,[2] A. Jungclaus,[11] D. Kameda,[2] G. D. Kim,[18] Y. K. Kim,[18,19] I. Kojouharov,[20] F. G. Kondev,[21] T. Kubo,[2] N. Kurz,[20] Y. K. Kwon,[18] G. J. Lane,[22] C.-B. Moon,[23] A. Montaner-Pizá,[24] K. Moschner,[25] F. Naqvi,[26] M. Niikura,[3] H. Nishibata,[13] D. Nishimura,[27] A. Odahara,[13] R. Orlandi,[28,‡] Z. Patel,[29] Zs. Podolyák,[29] H. Sakurai,[2] H. Schaffner,[20] G. S. Simpson,[8] K. Steiger,[17] H. Suzuki,[2] H. Takeda,[2] A. Wendt,[25] and K. Yoshinaga[27]

[1]*IRCNPC, School of Physics and Nuclear Energy Engineering, Beihang University, Beijing 100191, China*
[2]*RIKEN Nishina Center, 2-1 Hirosawa, Wako, Saitama 351-0198, Japan*
[3]*Department of Physics, University of Tokyo, Hongo, Bunkyo-ku, Tokyo 113-0033, Japan*
[4]*Center for Nuclear Study, University of Tokyo, Hongo, Bunkyo-ku, Tokyo 113-0033, Japan*
[5]*Department of Physics, Tohoku University, Aoba, Sendai, Miyagi 980-8578, Japan*
[6]*Department of Physics, Peking University, Beijing 100871, China*
[7]*School of Computing Engineering and Mathematics, University of Brighton, Brighton, BN2 4GJ, United Kingdom*
[8]*LPSC, Université Joseph Fourier Grenoble 1, CNRS/IN2P3, Institut National Polytechnique de Grenoble, F-38026 Grenoble Cedex, France*
[9]*Department of Physics, Chung-Ang University, Seoul 156-756, Republic of Korea*
[10]*Departamento de Física Teórica, Universidad Autónoma de Madrid, E-28049 Madrid, Spain*
[11]*Instituto de Estructura de la Materia, CSIC, E-28006 Madrid, Spain*
[12]*MTA Atomki, P.O. Box 51, Debrecen, H-4001, Hungary*
[13]*Department of Physics, Osaka University, Machikaneyama-machi 1-1, Osaka 560-0043 Toyonaka, Japan*
[14]*INFN, Sezione di Milano, via Celoria 16, I-20133 Milano, Italy*
[15]*Department of Physics, Sungkyunkwan University, Suwon 440-746, Republic of Korea*
[16]*Dipartimento di Fisica, Universitá di Milano, via Celoria 16, I-20133 Milano, Italy*
[17]*Physik Department, Technische Universität München, D-85748 Garching, Germany*
[18]*Rare Isotope Science Project, Institute for Basic Science, Daejeon 305-811, Republic of Korea*
[19]*Department of Nuclear Engineering, Hanyang University, Seoul 133-791, Republic of Korea*
[20]*GSI Helmholtzzentrum für Schwerionenforschung GmbH, 64291 Darmstadt, Germany*
[21]*Nuclear Engineering Division, Argonne National Laboratory, Argonne, Illinois 60439, USA*
[22]*Department of Nuclear Physics, R.S.P.E., Australian National University, Canberra, Australian Capital Territory 0200, Australia*
[23]*Department of Display Engineering, Hoseo University, Chung-Nam 336-795, Republic of Korea*
[24]*IFIC, CSIC-Universidad de Valencia, A.C. 22085, E 46071, Valencia, Spain*
[25]*Institut für Kernphysik, Universität zu Köln, Zülpicher Strasse 77, D-50937 Köln, Germany*
[26]*Wright Nuclear Structure Laboratory, Yale University, New Haven, Connecticut 06520-8120, USA*
[27]*Department of Physics, Faculty of Science and Technology, Tokyo University of Science, 2641 Yamazaki, Noda, Chiba, Japan*
[28]*Instituut voor Kern en Stralingsfysica, KU Leuven, University of Leuven, B-3001 Leuven, Belgium*
[29]*Department of Physics, University of Surrey, Guildford GU2 7XH, United Kingdom*

(Received 15 April 2014; published 25 July 2014)

A new isomer with a half-life of 23.0(8) ms has been identified at 2406 keV in ^{126}Pd and is proposed to have a spin and parity of 10^+ with a maximally aligned configuration comprising two neutron holes in the $1h_{11/2}$ orbit. In addition to an internal-decay branch through a hindered electric octupole transition, β decay from the long-lived isomer was observed to populate excited states at high spins in ^{126}Ag. The smaller energy difference between the 10^+ and 7^- isomers in ^{126}Pd than in the heavier $N = 80$ isotones can be interpreted as being ascribed to the monopole shift of the $1h_{11/2}$ neutron orbit. The effects of the monopole interaction on the evolution of single-neutron energies below ^{132}Sn are discussed in terms of the central and tensor forces.

DOI: 10.1103/PhysRevLett.113.042502 PACS numbers: 23.35.+g, 23.20.Lv, 23.40.−s, 27.60.+j

The nucleus, i.e., the highly dense central core of an atom, is an aggregate of two types of subatomic particles, protons and neutrons (nucleons). The stability of atomic nuclei, which is inherently linked to the presence of materials in nature, is much influenced by a shell structure and its resulting magic numbers; nuclei with specific numbers of nucleons (2, 8, 20, 28, 50, 82 for protons and, also, 126 for neutrons) near the β-stability line

necessitate relatively high energies to remove one or two nucleons compared to the neighboring isotopes. Such a situation is analogous to the noble gases that have large ionization energies with closed-shell configurations of electrons.

The traditional nuclear magic numbers, which have been the microscopic basis for understanding nuclear structure for half a century since Mayer and Jensen [1,2], are nowadays recognized as being one aspect of a more generalized concept of the shell structure that can vary as functions of the proton number (Z) or neutron number (N) [3]. One of the underlying causes for shell evolution is based on the strong monopole part of effective nucleon-nucleon interactions including the central and tensor forces, the latter of which plays an important role in the appearance or disappearance of the spherical magic numbers in light-mass nuclei with large N/Z ratios [4]. For heavier nuclei, similar mechanisms of the monopole interaction provide a reasonable explanation for the observed drift of single-particle levels along the $N = 51$ isotonic and the Sb ($Z = 51$) isotopic chains [5,6].

Concerning the $N = 82$ magicity, the recent spectroscopic study of ^{128}Pd ($Z = 46$, $N = 82$) revealed that this shell closure is so robust as to give rise to the seniority isomerism in the semimagic nucleus [7]. Meanwhile, a reduction of the $N = 82$ shell gap toward $Z = 40$ was suggested by mean-field and shell-model (SM) calculations [8,9]. To tackle this issue from a microscopic viewpoint, it is crucial to elucidate the properties of single-neutron states below the doubly magic nucleus ^{132}Sn ($Z = 50$, $N = 82$). The ordering of single-particle orbitals and their energies in the vicinity of ^{132}Sn are reviewed in Ref. [10]. Of particular interest is the behavior of the $1h_{11/2}$ neutron orbit that locates just below the $N = 82$ shell closure, hereby being significant for the reduction of the $N = 82$ shell gap as protons are removed from the $1g_{9/2}$ orbit in the $Z = 40$–50 subshell. In the present Letter, we focus on the characteristic isomers involving neutron-hole configurations with the $1h_{11/2}$ orbit in ^{126}Pd ($N = 80$). The systematic investigation of the analogous isomers in the $N = 80$ isotones uniquely embosses the evolution of this key orbit. This Letter presents, for the first time, an experimental implication for the monopole effects from the central and tensor forces on the shift of single-neutron energies below ^{132}Sn.

The knowledge of single-neutron states in this region also has a significant impact on the understanding of nucleosynthesis in the rapid neutron-capture (r) process [11], as the reaction rate of direct neutron capture after $(n,\gamma) \rightleftharpoons (\gamma,n)$ equilibrium, during the so-called freeze-out era, is expected to depend on the nature of single-neutron orbits around $N = 82$ [12]. Furthermore, the presence of isomeric states as long lived as the respective ground states in this neutron-rich region may affect the Solar System abundance distribution around the prominent $A \approx 130$ peak of the r-process isotopes.

Spectroscopic studies of ^{126}Pd have been performed at the RI Beam Factory (RIBF) facility [13], cooperated by RIKEN Nishina Center and CNS, University of Tokyo. Neutron-rich nuclei below ^{132}Sn were produced using in-flight fission of a $^{238}U^{86+}$ beam at 345 MeV/nucleon with the intensity ranging from 7 to 12 pnA, impinging on a beryllium target with a thickness of 3 mm. The nuclei of interest were separated and identified through the BigRIPS separator and the following ZeroDegree spectrometer [14]. A total of 5.3×10^4 ^{126}Pd fragments were implanted into a highly segmented active stopper, named WAS3ABi [15], which consisted of eight double-sided silicon-strip detectors (DSSSDs) stacked compactly. Each DSSSD had a thickness of 1 mm with an active area segmented into sixty and forty strips (1 mm pitch) on each side in the horizontal and vertical dimensions, respectively. The DSSSDs also served as detectors for electrons following β-decay and internal conversion (IC) processes. Gamma rays were detected by the EURICA array [16] that consisted of twelve Cluster-type detectors, each of which contained seven HPGe crystals packed closely. The γ-ray measurements were carried out with a time condition up to 100 μs relative to the trigger signal generated either from a plastic scintillation counter placed at the end of the beam line or from WAS3ABi.

Isomeric states with (sub)microsecond lifetimes were investigated by means of particle-γ (delayed) coincidence on an event-by-event basis [7]. Meanwhile, to study the decay of long-lived states in the millisecond range, the implantation of an identified particle was associated with the subsequent electron events that were detected in the DSSSD pixels where the beam particle was implanted. The result presented in this Letter was obtained using the latter analysis method.

The decay schemes of the isomeric states in ^{126}Pd are exhibited in Fig. 1. For ^{126}Pd, the $J^\pi = (5^-)$ and (7^-) isomers at 2023 and 2110 keV, respectively, were reported in Ref. [7]. In the present Letter, the γ rays below these isomers, except for the 86 keV line, have also been observed in coincidence with electrons that were associated with the prior implantation of ^{126}Pd, as demonstrated in Fig. 2(a). This observation implies the existence of a long-lived, higher-spin isomer which decays via the cascades that include electromagnetic transitions with relatively large total conversion coefficients (α_T). With gates on these γ rays, a prominent peak can be found in an electron spectrum [marked with "I" in the inset of Fig. 2(b)]; this corresponds to the conversion electrons for the 86 keV, $E2$ transition ($\alpha_T = 2.374$ [17]). In Fig. 2(b), a γ ray at 297 keV is clearly visible in addition to the γ rays below the (5^-) isomer by gating on the 86 keV IC peak. The appearance of the 297 keV peak is emphasized by taking a γ-ray time condition earlier than electron events, as is evident from the inset of Fig. 2(a), suggesting that this new γ ray precedes the highly converted 86 keV transition.

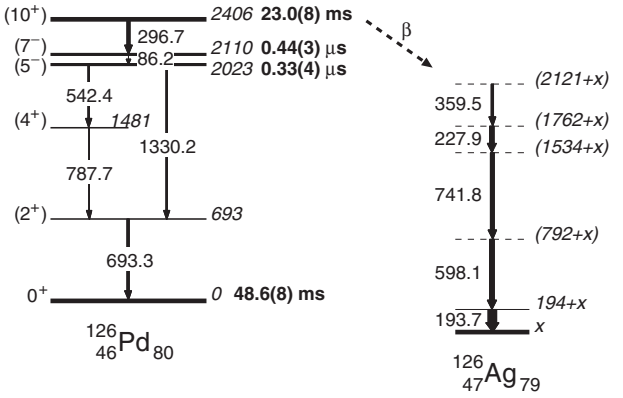

FIG. 1. Decay schemes of the $J^{\pi} = (10^{+})$ isomer in ^{126}Pd. The widths of arrows represent relative intensities of γ rays summarized in Table I, except for the 86 keV transition in ^{126}Pd. In ^{126}Ag, the order of transitions between the levels at $2121 + x$ and $194 + x$ keV, which are populated via the β decay of the (10^{+}) isomer, is ambiguous. (x denotes the unknown excitation energy of the lowest-lying state.)

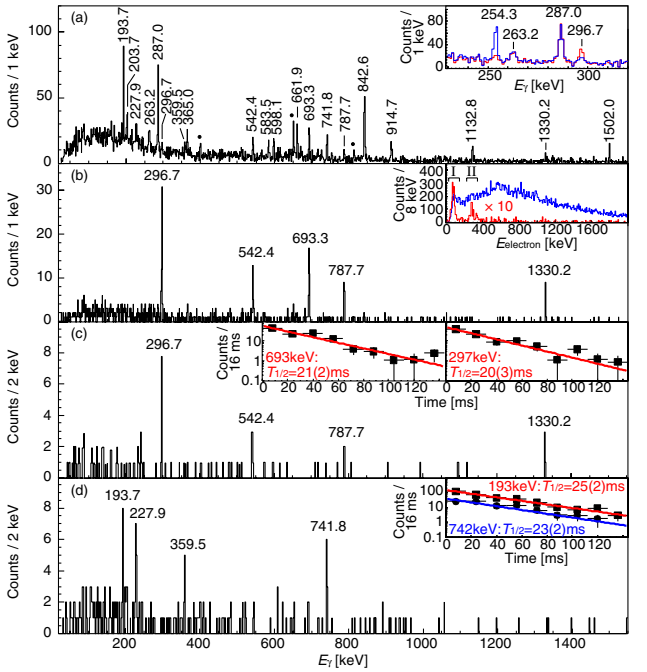

FIG. 2 (color online). (a) γ-ray spectrum measured within 50 ms after the ^{126}Pd implantation with a gate on an electron-γ time difference of $-0.5 \le \Delta t_{e\gamma} \le 0.5$ μs. Contaminants from the granddaughter ^{126}Cd are marked with filled circles. The inset magnifies the energy region from 230 to 310 keV measured with $-4.0 \le \Delta t_{e\gamma} \le 0.5$ μs (red) and $-0.5 \le \Delta t_{e\gamma} \le 50$ μs (blue). (b) γ rays measured with $-4.0 \le \Delta t_{e\gamma} \le 0.5$ μs, and additionally, with a gate on the electron peak marked with "I" in the inset, where the spectrum depicted with the red line (multiplied by a factor of 10) is obtained with a sum of gates on the γ rays below the (5^{-}) isomer in ^{126}Pd, while the blue line represents an electron spectrum without γ-ray gates. (c) and (d) γ-ray coincidence spectra measured by gating on the 693 and 598 keV γ rays, respectively. The insets show the time distributions of γ rays as indicated.

Furthermore, the 297 keV γ ray is observed in coincidence with the other γ rays in ^{126}Pd [see Fig. 2(c) as an example]. Thus, the long-lived isomer can be identified at an excitation energy of 2406 keV. A peak marked with "II" in the inset of Fig. 2(b) is expected to arise from the conversion electrons for the 297 keV transition, being most likely of an $E3$ character ($\alpha_T = 0.1197$ [17]).

The half-life ($T_{1/2}$) derived from the time distribution of the 297 keV γ ray is in agreement with that of the 693 keV one within experimental errors, as illustrated in the insets of Fig. 2(c). Similar half-lives have been observed for six other γ rays that are listed in the second group of Table I; these transitions are expected to belong to high-spin states in ^{126}Ag ($Z = 47$, $N = 79$) which are populated through the β decay of the long-lived isomer in ^{126}Pd. Therefore, the isomeric half-life is determined to be 23.0(8) ms by taking a weighted average of the respective values listed in the first and second groups of Table I. Based on the observed mutual coincidence [see Fig. 2(d)] and γ-ray intensities, we propose the decay scheme from the long-lived isomer in ^{126}Pd to the high-spin states in ^{126}Ag as shown in Fig. 1.

The γ rays following the β decay of the ground state of ^{126}Pd have also been observed in Fig. 2(a). Prior to the present work, an isomeric state with $J^{\pi} = (1^{-})$ was known at 254 keV in ^{126}Ag [18]. This isomeric transition is visible in our analysis of delayed coincidence with β rays, as shown in the inset of Fig. 2(a). The γ rays which show half-lives longer than the 23 ms isomer are summarized in the third group of Table I and assigned for low-spin states in ^{126}Ag. A weighted average of the respective fits leads to $T_{1/2} = 48.6(8)$ ms for the ground state in ^{126}Pd, which is consistent with the value extracted from an independent analysis of β-decay half-lives [19]. It is worth remarking that the isomer half-life is nearly half of that of the ground state.

A spin and parity of (10^{+}) was assigned for the $T_{1/2} = 23.0(8)$ ms isomeric state on the basis of the arguments as follows: Assuming that all the intensities of the β decay from the long-lived isomer flow into the 194 keV transition in ^{126}Ag, the number of γ-ray counts can be approximated as $N_{\gamma}(194) \approx Y \times R_{\text{ext}} \times \varepsilon_{\beta} \times \varepsilon_{\gamma}(194)$. Here, Y denotes the isomeric yield that can be calculated by multiplying the total number of the ^{126}Pd ions by the isomeric ratio, which is estimated to be 7.7(2)% from the population of the $J^{\pi} = (10^{+})$ isomer in ^{128}Cd [20] observed simultaneously in the present work. The γ-ray full-energy peak efficiency ε_{γ} is evaluated using ^{133}Ba and ^{152}Eu sources placed at the center of WAS3ABi, while $\varepsilon_{\beta} = 68(2)\%$ is derived from the ratio of the detected β events, which are associated predominately with the decay of the ^{126}Pd ground state, to the ^{126}Pd implants. The internal-decay branch, $R_{\text{int}} = 1 - R_{\text{ext}}$, can be estimated to be 28(8)% with the measured $N_{\gamma}(194)$. Meanwhile, R_{int} can be evaluated independently using the intensity of the 297 keV γ ray

TABLE I. Summary of transitions in ^{126}Pd and ^{126}Ag.

Parent J^π	Daughter	E_γ (keV)	$T_{1/2}$ (ms)	I_γ (%)
^{126}Pd, (10^+)	^{126}Pd	86.2	...	...
		296.7	20(3)	7.5(8)
		542.4	20(3)	4.1(6)
		693.3	21(2)	6.6(9)
		787.7	18(4)	3.8(5)
		1330.2	23(5)	3.5(8)
^{126}Pd, (10^+)	^{126}Ag, high spins	193.7	25(2)	26(3)
		203.7[a]	27(2)	11(2)
		227.9	27(10)	12(2)
		359.5	17(4)	7(2)
		598.1	26(3)	13(2)
		741.8	23(2)	12(2)
^{126}Pd, 0^+	^{126}Ag, low spins	254.3[a]	54(3)	52(4)
		263.2[a]	56(4)	21(3)
		287.0[a]	48(2)	68(4)
		365.0[a]	48(3)	30(3)
		583.5[a]	46(5)	17(3)
		661.9[a]	46(3)	35(3)
		842.6[a]	48(2)	100(6)
		914.7[a]	46(4)	30(3)
		1133.2[a]	52(4)	30(4)
		1502.0[a]	41(3)	27(4)

[a]Not incorporated in the level schemes of Fig. 1.

in ^{126}Pd as follows, $N_\gamma(297) \approx Y \times R_{\rm int} \times [\alpha_T(86)/1+\alpha_T(86)] \times \varepsilon_{\rm IC} \times [1/1+\alpha_T(297)] \times \varepsilon_\gamma(297)$. Given an $E3$ multipolarity for the 297 keV transition, $R_{\rm int} = 0.23(3)/\varepsilon_{\rm IC}$, being consistent with the value obtained above for $\varepsilon_{\rm IC} \gtrsim 60\%$. A transition strength of $B(E3) = 0.069(20)$ W.u. can be obtained for the 297 keV γ ray with $R_{\rm int} = 28(8)\%$. Such a hindered $E3$ transition from the analogous 10^+ isomer is known to be present also in ^{132}Te ($Z = 52$, $N = 80$) [21] and ^{132}Xe ($Z = 54$, $N = 78$) [22], as will be discussed later.

The main surprise in the present Letter is the small energy difference between the (10^+) and (7^-) isomers, $\Delta E_{7^-}^{10^+}$, in ^{126}Pd, compared to the analogous levels in the heavier $N = 80$ isotones, as demonstrated in Fig. 3(a). Since these two levels consist predominantly of maximally aligned two neutron-hole configurations, $(\nu 1h_{11/2}^{-2})_{10^+}$ and $(\nu 1h_{11/2}^{-1} 2d_{3/2}^{-1})_{7^-}$, their level energies depend on the single-particle energies (SPEs) of the $\nu 1h_{11/2}$ and $\nu 2d_{3/2}$ neutron orbits, as well as the strength of interactions between them. It can be seen in Fig. 3(a) that the energy of the $11/2^-$ level relative to the $3/2^+$ ground state in the neighboring $N = 81$ isotones decreases when approaching $Z = 50$. Note that these states are of one neutron-hole nature, and that the smooth reduction in energy can be essentially interpreted in terms of a short-range proton-neutron interaction [23] as follows: The $\pi 1g_{7/2}$ proton orbit lies just above the $Z = 50$ shell closure. The monopole interaction between $\pi 1g_{7/2}$ and $\nu 1h_{11/2}$, a spin-flip pair with $\Delta\ell = 1$ and $\Delta n = 0$, is

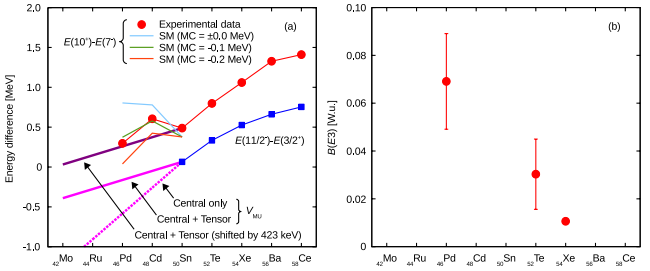

FIG. 3 (color online). (a) Energy differences between the 10^+ and 7^- states, $\Delta E_{7^-}^{10^+}$, in $N = 80$ (filled circles) and between the $11/2^-$ and $3/2^+$ states in $N = 81$ (filled squares). The data are taken from Ref. [25] for $Z \geq 50$, Ref. [20] for ^{128}Cd, and the present work for ^{126}Pd. For $Z \leq 50$, the differences in energy between the $1h_{11/2}$ and $2d_{3/2}$ neutron orbits calculated by $V_{\rm MU}$ interaction [6] and $\Delta E_{7^-}^{10^+}$ by SM calculations with monopole corrections (MC) are also depicted. (b) $B(E3; 10^+ \rightarrow 7^-)$ values in $^{126}_{46}$Pd, $^{132}_{52}$Te [21], and $^{132}_{56}$Xe [22].

stronger than the $\pi 1g_{7/2}$-$\nu 2d_{3/2}$ pair, due to the larger overlap between the radial wave functions of the two orbits. Therefore, when emptying the $\pi 1g_{7/2}$ subshell, the $\nu 1h_{11/2}$ orbit is relatively less bound than the $\nu 2d_{3/2}$ one. The moderation in the slope at higher Z may be ascribed to the partial occupation of the $\pi 2d_{5/2}$ orbit, which exerts a weaker (stronger) monopole interaction on the $\nu 1h_{11/2}$ ($\nu 2d_{3/2}$) neutrons than $\pi 1g_{7/2}$. As is evident from the comparison in Fig. 3(a), a similar trend is observed for $\Delta E_{7^-}^{10^+}$. This finding supports that these isomers can serve as sensitive probes for the evolution of the constituent neutron shell orbits.

Below $Z = 50$, protons in the $\pi 1g_{9/2}$ subshell play a major role in changing the neutron SPEs, because this orbit is near the Fermi surface. The neutron SPEs are estimated by the monopole-based universal interaction, $V_{\rm MU}$, which consists of the Gaussian central force and the tensor force based on the $\pi + \rho$ meson exchanges, using the parameters fixed in Ref. [6]. The $V_{\rm MU}$ interaction has been applied to other regions of exotic nuclei and successfully reproduced various types of the shell evolution [6]. Figure 3(a) shows the evolutions of the relative $11/2^-$ energy starting from the experimental value in ^{131}Sn, predicted by the $V_{\rm MU}$ calculation with $A = 130$. In the calculation, the $\pi 1g_{9/2}$ subshell is considered to be well isolated between $Z = 50$ and 40. In Fig. 3(a), only with the central force the $11/2^-$ energy rapidly decreases to negative values as the proton number decreases, indicating that the $\nu 1h_{11/2}$ orbit moves away from the $\nu 2d_{3/2}$ one towards the $N = 82$ gap. If there is the tensor force effect, however, the slope becomes less steep. The observed reduction in $\Delta E_{7^-}^{10^+}$ from ^{130}Sn to ^{126}Pd is consistent with the expectation of $V_{\rm MU}$ including both the central and tensor forces, given the same trend as the $11/2^-$ relative energies. Based on these findings, it can be concluded that the tensor force slows down the upward drift of the $\nu 1h_{11/2}$ SPE when protons are removed from the $\pi 1g_{9/2}$ orbit below ^{132}Sn.

One can notice a kink in the systematics of $\Delta E_{7^-}^{10^+}$ at ^{128}Cd in Fig. 3(a). It should be noted that the above V_{MU} calculation is based on the monopole properties of the proton-neutron interactions. While the overall trend can be accounted for by V_{MU}, other multipole components have to be introduced in a shell-model framework to describe the details of the level evolution. To confirm the effect of configuration mixing, a SM study based on the j-j coupling scheme was performed independently of the V_{MU} calculation. With the doubly magic nucleus ^{132}Sn as a closed core, the model space adopted includes the $2d_{3/2}$, $1h_{11/2}$, $3s_{1/2}$, $2d_{5/2}$, and $1g_{7/2}$ orbits for neutron holes, and the $1g_{9/2}$, $2p_{1/2}$, $2p_{3/2}$, and $1f_{5/2}$ orbits for proton holes. The SPEs were taken from the experimentally known levels in the single-hole nuclei, ^{131}Sn [24] and ^{131}In [9,26,27]. The surface-delta interaction (SDI) was employed for the proton-proton and neutron-neutron interactions, which were adjusted to reproduce the observed level energies of ^{130}Cd and ^{130}Sn, respectively. The proton-neutron two-body matrix elements (TBMEs) were derived from the empirical parametrization of interaction potentials [28]. For the $\pi 1g_{9/2}$-$\nu 1h_{11/2}$ multiplet, the monopole correction was introduced by adding a constant to the diagonal TBME.

The results of SM calculations with different values of the monopole correction for $Z \leq 50$ are displayed in Fig. 3(a). The kink manifests in the calculated $\Delta E_{7^-}^{10^+}$, as well as in the experimental result. Moreover, it can be seen that the variation in $\Delta E_{7^-}^{10^+}$ is very sensitive to the value of the monopole correction. According to the present SM calculation, the wave functions of the 10^+ and 7^- states in each $N = 80$ isotone are scarcely affected by the monopole corrections. These arguments indicate that the lowering of $\Delta E_{7^-}^{10^+}$ in ^{126}Pd is ascribed to the monopole effect between the $\pi 1g_{9/2}$ and $\nu 1h_{11/2}$ orbitals rather than the configuration mixing of any kind.

Finally, it is worth commenting on the $E3$ transition depopulating the 10^+ isomeric state. If the 10^+ and 7^- isomers had pure two neutron-hole configurations, $\nu 1h_{11/2}^{-2}$ and $\nu 1h_{11/2}^{-1}2d_{3/2}^{-1}$, respectively, an $E3$ decay would not occur between them. A possible explanation for the measured large hindrance, $B(E3; 10^+ \rightarrow 7^-) = 0.069(20)$ W.u., may be given in terms of a small admixture of different multiplets. In general, transition strengths are more susceptible to the configuration mixing than level energies. As can be inferred from the drift of the neutron SPEs observed for the $N = 51$ isotones with $Z = 40 - 50$ [29], the $\nu 1g_{7/2}$ orbit is expected to be rapidly pushed up as removing the $\pi 1g_{9/2}$ protons, in consequence of the strong (attractive) monopole interaction between the spin-orbit partner. In Fig. 3(b), the observed rise in $B(E3; 10^+ \rightarrow 7^-)$ with decreasing proton number may suggest the admixture of different multiplets including the $\nu 1g_{7/2}$ hole, such as $\nu 1h_{11/2}^{-1}1g_{7/2}^{-1}$, in the 7^- state, to which the 10^+ isomer decays. [The aforementioned SM calculation predicts that the wave function of the 7^- state contains such kind of configurations by ~2.6%.] This hypothesis, based on the monopole migration, will be verified experimentally by identifying the $7/2^+$ hole states in the $N = 81$ isotones, which can be populated in the β decay of odd-mass $N = 82$ nuclei through the $\nu 1g_{7/2} \rightarrow \pi 1g_{9/2}$ Gamow-Teller transition.

In conclusion, a new isomeric state with $J^\pi = (10^+)$, $T_{1/2} = 23.0(8)$ ms has been identified at 2406 keV in ^{126}Pd. The long lifetime, which is about half $T_{1/2}$ of the ground state, allows the β decay to compete with a hindered $E3$ transition. The energy difference between the 10^+ and 7^- isomeric levels is smaller in ^{126}Pd than in the heavier $N = 80$ isotones, being qualitatively explained by the proton-neutron monopole interaction that includes the central- and tensor-force effects. This result indicates that the tensor force suppresses the drift of the $\nu 1h_{11/2}$ neutron orbit towards the $N = 82$ gap when protons are removed from the $\pi 1g_{9/2}$ subshell. Based on shell-model calculations with monopole corrections, we revealed that the energy shift of the 10^+ isomer is caused by the monopole part of the $\pi 1g_{9/2}$-$\nu 1h_{11/2}$ interaction, but not by the configuration mixing.

Probing the nature of single-neutron states not only below but also above the $N = 82$ shell gap is essential to pin down whether the shell quenching takes place in this neutron-rich region. The knowledge about neutron orbitals obtained in the present Letter will prompt further study of the single-neutron states by means of β-decay and transfer-reaction experiments using radioactive-isotope beams.

We thank the staff at RIBF for providing the beams, the EUROBALL Owners Committee for the loan of germanium detectors, the PreSpec Collaboration for the use of the readout electronics. Part of the WAS3ABi was supported by the Rare Isotope Science Project which is funded by MSIP and NRF of Korea. This work was supported by the Priority Centers Research Program in Korea (Contract No. 2009-0093817), OTKA Contract No. K100835, the U.S. DOE, Office of Nuclear Physics (Contract No. DE-AC02-06CH11357), NRF-2012R1A1A1041763, the Spanish Ministerio de Ciencia e Innovación (Grants No. FPA2009-13377-C02 and No. FPA2011-29854-C04), the European Commission through the Marie Curie Actions call FP7-PEOPLE-2011-IEF (Contract No. 300096), German BMBF under Contract No: 05P12PKFNE, and JSPS KAKENHI Grants No. 24740188 and No. 25247045. We thank Professor K. Kaneko and Y. Sun for valuable discussions on shell-model calculations.

*Corresponding author.hiroshi@ribf.riken.jp
†Department of Physics, University of Notre Dame, Notre Dame, Indiana 46556, USA.
‡Advanced Science Research Center, Japan Atomic Energy Agency, Tokai, Ibaraki, 319-1195, Japan.

[1] M. G. Mayer, Phys. Rev. **75**, 1969 (1949).
[2] O. Haxel, J. H. D. Jensen, and H. E. Suess, Phys. Rev. **75**, 1766 (1949).
[3] O. Sorlin and M.-G. Porquet, Prog. Part. Nucl. Phys. **61**, 602 (2008).
[4] T. Otsuka, R. Fujimoto, Y. Utsuno, B. A. Brown, M. Honma, and T. Mizusaki, Phys. Rev. Lett. **87**, 082502 (2001).
[5] T. Otsuka, T. Suzuki, R. Fujimoto, H. Grawe, and Y. Akaishi, Phys. Rev. Lett. **95**, 232502 (2005).
[6] T. Otsuka, T. Suzuki, M. Honma, Y. Utsuno, N. Tsunoda, K. Tsukiyama, and M. Hjorth-Jensen, Phys. Rev. Lett. **104**, 012501 (2010).
[7] H. Watanabe *et al.*, Phys. Rev. Lett. **111**, 152501 (2013).
[8] J. Dobaczewski, W. Nazarewicz, T. R. Werner, J. F. Berger, C. R. Chinn, and J. Dechargé, Phys. Rev. C **53**, 2809 (1996).
[9] J. Taprogge *et al.*, Phys. Rev. Lett. **112**, 132501 (2014).
[10] H. Grawe, K. Langanke, and G. Martnez-Pinedo, Rep. Prog. Phys. **70**, 1525 (2007).
[11] E. M. Burbidge, G. R. Burbidge, W. A. Fowler, and F. Hoyle, Rev. Mod. Phys. **29**, 547 (1957).
[12] T. Rauscher, R. Bieber, H. Oberhummer, K.-L. Kratz, J. Dobaczewski, P. Möller, and M. M. Sharma, Phys. Rev. C **57**, 2031 (1998).
[13] Y. Yano, Nucl. Instrum. Methods Phys. Res., Sect. B **261**, 1009 (2007).
[14] T. Kubo, Nucl. Instrum. Methods Phys. Res., Sect. B **204**, 97 (2003).
[15] S. Nishimura, Prog. Theor. Exp. Phys. 03C006 (2012).
[16] P.-A. Söderström *et al.*, Nucl. Instrum. Methods Phys. Res., Sect. B **317**, 649 (2013).
[17] T. Kibédi, T. W. Burrows, M. B. Trzhaskovskaya, P. M. Davidson, and C. W. Nestor, Nucl. Instrum. Methods Phys. Res., Sect. A **589**, 202 (2008).
[18] S. Lalkovski *et al.*, Phys. Rev. C **87**, 034308 (2013).
[19] G. Lorusso (to be published).
[20] L. Cáceres *et al.*, Phys. Rev. C **79**, 011301 (2009).
[21] J. Genevey, J. A. Pinston, C. Foin, M. Rejmund, R. F. Casten, H. Faust, and S. Oberstedt, Phys. Rev. C **63**, 054315 (2001).
[22] A. Kerek, A. Luukko, M. Grecescu, and J. Sztarkier, Nucl. Phys. **A172**, 603 (1971).
[23] L. Silverberg, Nucl. Phys. **60**, 483 (1964).
[24] B. Fogelberg, H. Gausemel, K. A. Mezilev, P. Hoff, H. Mach, M. Sanchez-Vega, A. Lindroth, E. Ramström, J. Genevey, J. A. Pinston, and M. Rejmund, Phys. Rev. C **70**, 034312 (2004).
[25] http://www.nndc.bnl.gov/ensdf/.
[26] A. Kankainen *et al.*, Phys. Rev. C **87**, 024307 (2013).
[27] M. Hannawald *et al.* (ISOLDE Collaboration), Phys. Rev. C **62**, 054301 (2000).
[28] J. P. Schiffer and W. W. True, Rev. Mod. Phys. **48**, 191 (1976).
[29] D. Seweryniak *et al.*, Phys. Rev. Lett. **99**, 022504 (2007).